PERGAMON

International Journal of Solids and Structures 38 (2001) 7409–7421

INTERNATIONAL JOURNAL OF SOLIDS and STRUCTURES

www.elsevier.com/locate/ijsolstr

Nonlinear analysis of functionally graded plates and shallow shells

J. Woo, S.A. Meguid *

Engineering Mechanics and Design Laboratory, Department of Mechanical and Industrial Engineering, University of Toronto, 5 King's College Road, Toronto, Ont., Canada M5S 3G8

Received 27 July 2000

Abstract

In this paper, an analytic solution is provided for the coupled large deflection of plates and shallow shells made of functionally graded materials (FGMs) under transverse mechanical loads and a temperature field. The material properties of the functionally graded shells are assumed to vary continuously through the thickness of the shell, according to a power law distribution of the volume fraction of the constituents. The fundamental equations for thin rectangular shallow shells of FGM are obtained using the von Karman theory for large transverse deflection, and the solution is obtained in terms of Fourier series. The effect of material properties, shell geometry and thermomechanical loading on the stress field are determined and discussed. The results reveal that thermomechanical coupling effects play a major role in dictating the response of the functionally graded shell.

Keywords: Functionally graded material; Shallow shells; Nonlinear analysis

1. Introduction

The concept of functionally graded materials (FGMs) was first introduced in 1984 by a group of material scientists in Japan, as ultrahigh temperature resistant materials for aircraft, space vehicles and other engineering applications. Since then, FGMs have attracted much interest as heat-shielding materials. FGMs are heterogeneous composite materials, in which the material properties vary continuously from one interface to the other. This is achieved by gradually varying the volume fraction of the constituent materials. The advantage of using these materials is that they can survive environments with high temperature gradients, while maintaining their structural integrity.

In view of the advantages of FGMs, a number of investigations dealing with thermal stresses had been published in the scientific literature. In recent years, Tanaka et al. (1993) studied an improved solution to thermoelastic material design in FGMs in order to reduce thermal stresses. Obata and Noda (1994)

* Corresponding author. Tel.: +1-416-978-5741; fax: +1-416-978-7753.
E-mail address: meguid@mie.utoronto.ca (S.A. Meguid).

0020-7683/01/$ - see front matter
PII: S0020-7683(01)00048-8

investigated the steady state thermal stress field in a hollow circular cylinder and a hollow sphere of a functionally graded material. Ishikawa (1990) analyzed the thermal deformation and thermal stresses of FGM plates under steady graded temperature field. Takezono et al. (1996) formulated analytically and numerically the thermal stress and deformation states for axisymmetrical shells of functionally graded material subjected to thermal loading due to a fluid. Wetherhold et al. (1996) considered the use of FGMs to eliminate or control thermal deformation in beams and plates. Praveen and Reddy (1998) investigated the response of functionally graded ceramic-metal plates using a plate finite element that accounts for the transverse shear strains, rotary inertia and moderately large rotations in the von Karman sense. The static and dynamic response of the functionally graded plates was investigated by varying the volume fraction of the ceramic and metallic constituents using a simple power law distribution. The effect of the imposed temperature field on the response of the FGM plate was also discussed. Loy et al. (1999) studied the vibration of cylindrical shells made of a functionally graded material compound of stainless steel and nickel. The objective was to investigate the influence of the constituent volume fractions and the configuration of the constituent materials on the natural frequency. The analysis was carried out with strain–displacement relations from Love's thin shell theory, and the eigenvalue equations were obtained using Rayleigh–Ritz method without temperature effects. Feldman and Aboudi (1997) studied elastic bifurcation buckling of functionally graded plates under in-plane compressive loading. In this work, they assumed that the grades of material properties throughout the structure are produced by a spatial distribution of the local reinforcement volume fraction $v_f = v_f(x, y, z)$. Considerable research has also been performed on the analysis of the thermal stresses and deformation of functionally graded structures. However, these studies were limited either to linear analysis, or to simplified nonlinear models.

In this work, the large deflection of functionally graded plates and shallow shells under transverse loading and temperature field is studied. The governing equations for thin rectangular shallow shells of FGMs are obtained using the von Karman theory, which considers moderate deflections and small strains. The material properties of functionally graded shells are assumed to vary continuously through the thickness of the shell, according to a power law distribution of the volume fraction of the constituents. A series solution is used to solve the coupled governing equations under simply supported boundary conditions. Numerical results are provided to show the influence of material properties, shell geometry, mechanical loading and a temperature field on the resulting stress state. The importance of our work is self evident in the design of thermal barrier coatings.

2. Fundamental equations

Shallow shells are assumed to have a relative small rise as compared with their spans. A rectangular shallow shell made of FGM is considered here. Let the xy plane of the xyz Cartesian coordinates overlap the rectangular plane area of the shell, as shown in Fig. 1. The middle surface of the shell is defined, in terms of curvilinear coordinates α and β, by the relations

$$\begin{aligned} x &= x(\alpha, \beta) \\ y &= y(\alpha, \beta) \\ z &= z(\alpha, \beta) \end{aligned} \tag{1}$$

For shallow thin shells, the displacements are assumed to take the following form:

$$\begin{aligned} u^* &= u(\alpha, \beta) - \xi w_{,\alpha} \\ v^* &= v(\alpha, \beta) - \xi w_{,\beta} \\ w^* &= w(\alpha, \beta) \end{aligned} \tag{2}$$

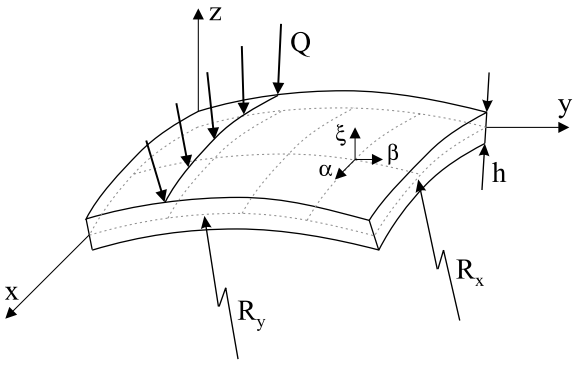

Fig. 1. Geometry and coordinates of a rectangular shallow shell.

where u^*, v^* and w^* are the total displacements, and u, v and w are the middle surface displacements in the α, β and ξ directions, respectively. The shell is said to be shallow, if $(\partial z/\partial x)^2$ and $(\partial z/\partial y)^2$ can be neglected by virtue of smallness in comparison to unity (Gould, 1977). Therefore, the xy Cartesian coordinates can replace the α and β curvilinear coordinates on the middle surface. The von Karman theory for moderately large deflections and small strains makes use of the nonlinear strain-displacement relations, in which quadratic terms in the slopes $w_{,x}$ and $w_{,y}$ are retained, while all other nonlinear terms are neglected. Therefore, the strains can be expressed as:

$$\{\varepsilon\} = \begin{Bmatrix} \varepsilon_x \\ \varepsilon_y \\ \gamma_{xy} \end{Bmatrix} = \begin{Bmatrix} \varepsilon_x^0 + \xi\kappa_x \\ \varepsilon_y^0 + \xi\kappa_y \\ \gamma_{xy}^0 + \xi\kappa_{xy} \end{Bmatrix} \tag{3}$$

in which the middle surface strains $\{\varepsilon\}$ is given by

$$\{\varepsilon^0\} = \begin{Bmatrix} \varepsilon_x^0 \\ \varepsilon_y^0 \\ \gamma_{xy}^0 \end{Bmatrix} = \begin{Bmatrix} u_{,x} + 1/2w_{,x}^2 + w/R_x \\ v_{,y} + 1/2w_{,y}^2 + w/R_y \\ u_{,y} + v_{,x} + w_{,x}w_{,y} + 2w/R_{xy} \end{Bmatrix} \tag{4}$$

while the curvature $\{\kappa\}$ is given by

$$\{\kappa\} = \begin{Bmatrix} \kappa_x \\ \kappa_y \\ \kappa_{xy} \end{Bmatrix} = \begin{Bmatrix} -w_{,xx} \\ -w_{,yy} \\ -2w_{,xy} \end{Bmatrix} \tag{5}$$

where R_x, R_y and R_{xy} are radii of curvature of the middle surface.

The plates and shallow shells of the FGM considered are assumed to be of uniform thickness h. The material properties P of the functionally graded shells are also assumed to vary through the thickness of the shell, as a function of the volume fraction and properties of the constituent materials. These properties can be expressed as

$$P = \sum_{j=1}^{k} P_j V_j \tag{6}$$

where P_j and V_j are the material property and volume fraction of the constituent material j. The volume fraction of all the constituent materials should add up to one,

$$\sum_{j=1}^{k} V_j = 1 \tag{7}$$

For a shell with a uniform thickness h and a reference surface at its middle surface, the volume fraction can be written as

$$V_j = \left(\frac{2\xi + h}{2h}\right)^n \tag{8}$$

where n is the power-law exponent, $0 \leqslant n \leqslant \infty$. For a functionally graded solid with two constituent materials, the property variation P can be expressed as

$$P(z) = (P_u - P_l)\left(\frac{2\xi + h}{2h}\right)^n + P_l \tag{9}$$

where P_u and P_l are the corresponding properties of the upper and lower surfaces. This power law assumption, which is widely accepted, reflects a simple rule of mixtures used to obtain the effective properties of FGMs (Praveen and Reddy, 1998). Therefore, the material properties along the thickness of the shells, such as Young's modulus $E(\xi)$, Poisson's ratio $v(\xi)$, and coefficient of thermal expansion $\alpha(\xi)$, can be determined according to Eq. (9). With the help of these material properties, the stresses can be determined as,

$$\begin{aligned}\{\sigma\} = \begin{Bmatrix}\sigma_x \\ \sigma_y \\ \tau_{xy}\end{Bmatrix} &= \frac{E(\xi)}{1-v^2(\xi)}\begin{bmatrix}1 & v(\xi) & 0 \\ v(\xi) & 1 & 0 \\ 0 & 0 & (1-v(\xi))/2\end{bmatrix}\begin{Bmatrix}\varepsilon_x \\ \varepsilon_y \\ \gamma_{xy}\end{Bmatrix} - \begin{Bmatrix}\frac{E(\xi)}{1-v(\xi)}\alpha(\xi)\Delta T(x,y,\xi) \\ \frac{E(\xi)}{1-v(\xi)}\alpha(\xi)\Delta T(x,y,\xi) \\ 0\end{Bmatrix} \\ &= [Q]\{\varepsilon\} - \begin{Bmatrix}\frac{E(\xi)}{1-v(\xi)}\alpha(\xi)\Delta T(x,y,\xi) \\ \frac{E(\xi)}{1-v(\xi)}\alpha(\xi)\Delta T(x,y,\xi) \\ 0\end{Bmatrix}\end{aligned} \tag{10}$$

where $E(\xi)$, $v(\xi)$, $\alpha(\xi)$ and $\Delta T(x,y,\xi)$ are Young's modulus, Poisson's ratio, coefficient of linear thermal expansion, and temperature referenced to the stress free state, respectively.

The axial force N and moment M can be calculated using the following expression,

$$(N_{\alpha\beta}, M_{\alpha\beta}) = \int_{-h/2}^{h/2} (1, \xi)\sigma_{\alpha\beta}\,\mathrm{d}\xi \tag{11}$$

where α and β stand for x and y. Hence, we have

$$\begin{aligned}\{N\} &= [A]\{\varepsilon^0\} + [B]\{\kappa\} - \{N^T\} \\ \{M\} &= [B]\{\varepsilon^0\} + [D]\{\kappa\} - \{M^T\}\end{aligned} \tag{12}$$

in which $[A]$, $[B]$ and $[D]$ are the respective in-surface, bending–stretching coupling and bending stiffness, and are given by

$$([A],[B],[D]) = \int_{-h/2}^{h/2} (1, \xi, \xi^2)[Q]\,\mathrm{d}\xi \tag{13}$$

and the thermal force N^T and thermal moment M^T are given by

$$\{N^T\} = \begin{Bmatrix}N_x^T \\ N_y^T \\ 0\end{Bmatrix} = \begin{Bmatrix}\int_{-h/2}^{h/2} \frac{E}{1-v}\alpha\Delta T\,\mathrm{d}\xi \\ \int_{-h/2}^{h/2} \frac{E}{1-v}\alpha\Delta T\,\mathrm{d}\xi \\ 0\end{Bmatrix}, \qquad \{M^T\} = \begin{Bmatrix}M_x^T \\ M_y^T \\ 0\end{Bmatrix} = \begin{Bmatrix}\int_{-h/2}^{h/2} \frac{E}{1-v}\alpha\Delta T\xi\,\mathrm{d}\xi \\ \int_{-h/2}^{h/2} \frac{E}{1-v}\alpha\Delta T\xi\,\mathrm{d}\xi \\ 0\end{Bmatrix} \tag{14}$$

If Airy's stress function φ is introduced such that,

$$N_x = \varphi_{,yy}, \quad N_y = \varphi_{,xx}, \quad N_{xy} = -\varphi_{,xy} \tag{15}$$

then the governing equations can be reduced to

$$\begin{aligned}
&a_{22}\varphi_{,xxxx} + (2a_{12} + a_{33})\varphi_{,xxyy} + a_{11}\varphi_{,yyyy} = f_1 + f_1' - f_1^{\mathrm{T}} \\
&d_{11}w_{,xxxx} + (2d_{12} + d_{33})w_{,xxyy} + d_{22}w_{,yyyy} = q + f_2 + f_2' - f_2^{\mathrm{T}} \\
&f_1 = w_{,xy}^2 - w_{,xx}w_{,yy} + w_{,yy}/R_x + w_{,xx}/R_y - 2w_{,xy}/R_{xy} \\
&f_1' = -[b_{12}w_{,xxxx} + (b_{11} + b_{22} - 2b_{33})w_{,xxyy} + b_{12}w_{,yyyy}] \\
&f_1^{\mathrm{T}} = a_{12}N_{x,xx}^{\mathrm{T}} + a_{11}N_{x,yy}^{\mathrm{T}} + a_{22}N_{y,xx}^{\mathrm{T}} + a_{12}N_{y,yy}^{\mathrm{T}} \\
&f_2 = \varphi_{,yy}(w_{,xx} - 1/R_x) + \varphi_{,xx}(w_{,yy} - 1/R_y) - 2\varphi_{,xy}(w_{,xy} - 1/R_{xy}) \\
&f_2' = c_{12}\varphi_{,xxxx} + (c_{11} + c_{22} - 2c_{33})\varphi_{,xxyy} + c_{12}\varphi_{,yyyy} \\
&f_2^{\mathrm{T}} = M_{x,xx}^{\mathrm{T}} + M_{y,yy}^{\mathrm{T}} \\
&[a] = [A]^{-1} \\
&[b] = [A]^{-1}[B] \\
&[c] = [B][A]^{-1} \\
&[d] = [D] - [B][A]^{-1}[B]
\end{aligned} \tag{16}$$

where the first two terms and the last three terms of f_1 represent the effects of von Karman nonlinear theory and the initial curvature of the shallow shell, respectively. f_2 also contains the nonlinear as well as the curvature terms. f_2' represents the effect of membrane-bending coupling due to unsymmetrical material property distribution along the thickness and f_1^{T} and f_2^{T} represent thermal loads.

Consider now the case of a simply supported shell. In this case, the boundary conditions are

$$\begin{aligned}
&x = 0, a: \quad N_x = \varphi_{,yy} = 0, \quad N_{xy} = -\varphi_{,xy} = 0, \quad w = 0, \quad M_x = 0 \\
&y = 0, b: \quad N_y = \varphi_{,xx} = 0, \quad N_{xy} = -\varphi_{,xy} = 0, \quad w = 0, \quad M_y = 0
\end{aligned} \tag{17}$$

Let us introduce the following dimensionless variables,

$$\begin{aligned}
&\lambda = a/b, \quad \zeta = x/a, \quad \eta = y/b \\
&W = w/h \\
&\Phi = \varphi/d_{11} + P(\eta^2 + \rho\lambda^2\zeta^2)/(2\lambda^2), \quad P = -a^2N_x^0/d_{11}, \quad \rho = N_y^0/N_x^0 \\
&Q = a^4q/(d_{11}h) \\
&M_\zeta^{\mathrm{T}} = a^2M_x^{\mathrm{T}}/(d_{11}h), \quad M_\eta^{\mathrm{T}} = a^2M_y^{\mathrm{T}}/(d_{11}h), \quad N_\zeta^{\mathrm{T}} = a^2N_x^{\mathrm{T}}/(d_{11}h), \quad N_\eta^{\mathrm{T}} = a^2N_y^{\mathrm{T}}/(d_{11}h) \\
&R = R_xh/a^2, \quad r = R_x/R_y, \quad r_1 = R_x/R_{xy} \\
&v_d = (d_{12} + 2d_{33})/d_{11}, \quad v_a = (a_{12} + 2a_{33})/a_{11}, \quad v_b = (b_{11} - b_{33})/b_{12} \\
&\varepsilon_b = b_{11}/h, \quad \varepsilon_a = h^2/(a_{11}d_{11}) \\
&\delta_{b12} = b_{12}/b_{11}, \quad \delta_{b33} = b_{33}/b_{11}, \quad \delta_{a12} = a_{12}/a_{11}
\end{aligned} \tag{18}$$

With the help of these dimensionless variables, the governing equations and boundary conditions become,

$$
\begin{aligned}
&\Phi_{,\zeta\zeta\zeta\zeta} + 2v_a\lambda^2\Phi_{,\zeta\zeta\eta\eta} + \lambda^4\Phi_{,\eta\eta\eta\eta} = \varepsilon_a(F_1 - \varepsilon_b F_1') - Q_N \\
&W_{,\zeta\zeta\zeta\zeta} + 2v_d\lambda^2 W_{,\zeta\zeta\eta\eta} + \lambda^4 W_{,\eta\eta\eta\eta} = Q + F_2 + \varepsilon_b F_2' - Q_M \\
&F_1 = \lambda^2 W_{,\zeta\eta}^2 - \lambda^2 W_{,\zeta\zeta}W_{,\eta\eta} + \lambda^2 W_{,\eta\eta}/R + W_{,\zeta\zeta}r/R - 2\lambda W_{,\zeta\eta}r_1/R \\
&F_1' = \delta_{b12}(W_{,\zeta\zeta\zeta\zeta} + 2v_b\lambda^2 W_{,\zeta\zeta\eta\eta} + \lambda^4 W_{,\eta\eta\eta\eta}) \\
&Q_N = \delta_{a12}N^{\mathrm{T}}_{\zeta,\zeta\zeta} + \lambda^2 N^{\mathrm{T}}_{\zeta,\eta\eta} + N^{\mathrm{T}}_{\eta,\zeta\zeta} + \delta_{a12}N^{\mathrm{T}}_{\eta,\eta\eta} \\
&F_2 = \lambda^2\Phi_{,\eta\eta}(W_{,\zeta\zeta} - 1/R) + \Phi_{,\zeta\zeta}(\lambda^2 W_{,\zeta\zeta} - r/R) - 2\lambda\Phi_{,\zeta\eta}(W_{,\zeta\eta} - r_1/R) \\
&F_2' = \delta_{b12}(\Phi_{,\zeta\zeta\zeta\zeta} + 2v_b\lambda^2\Phi_{,\zeta\zeta\eta\eta} + \lambda^4\Phi_{,\eta\eta\eta\eta}) \\
&Q_M = M^{\mathrm{T}}_{\zeta,\zeta\zeta} + \lambda^2 M^{\mathrm{T}}_{\eta,\eta\eta} \\
&\zeta = 0,1: \quad \Phi_{,\eta\eta} = 0, \quad \Phi_{,\zeta\eta} = 0, \quad W = 0, \quad W_{,\zeta\zeta} = \varepsilon_b N^{\mathrm{T}}_{\zeta} - M^{\mathrm{T}}_{\zeta} \\
&\eta = 0,1: \quad \Phi_{,\zeta\zeta} = 0, \quad \Phi_{,\zeta\eta} = 0, \quad W = 0, \quad W_{,\eta\eta} = (\varepsilon_b N^{\mathrm{T}}_{\eta} - M^{\mathrm{T}}_{\eta})/\lambda^2
\end{aligned}
\tag{19}
$$

which are treated in the next section. When R in the Eq. (9) becomes infinity, the equation reduces to the governing equation of the plate.

Let us now consider the influence of a temperature field on the behavior of the composite FGM. It is assumed that one value of the temperature is imposed on the upper surface and the other value on the lower surface. This one dimensional temperature field is assumed to be constant in the plane of the plate. In this case, the temperature distribution along the thickness can be obtained by solving a simple steady state heat transfer equation through the thickness of the plate. The equation for the temperature through the thickness is given by

$$-(k(z)T'(z))' = 0 \tag{20}$$

where $T = T_{\mathrm{u}}$ at $z = h/2$ and $T = T_{\mathrm{l}}$ at $z = -h/2$, the thermal conductivity $k(z)$ is also assumed to vary according to Eq. (9). The solution to Eq. (20) is

$$T(z) = T_{\mathrm{u}} - \frac{T_{\mathrm{u}} - T_{\mathrm{l}}}{\int_{-h/2}^{h/2}\frac{\mathrm{d}z}{k(z)}}\int_{-h/2}^{z}\frac{\mathrm{d}z}{k(z)} \tag{21}$$

This equation does not take into consideration the temperature dependence of the material properties. As indicated in the work by Miyamoto (1999), this will not have a significant effect on results. The thermal force N^{T} and thermal moment M^{T} can be calculated using Eq. (14) after the temperature field distribution has been obtained by integrating Eq. (21).

3. Solution of governing equations

Assume that a solution of W and Φ can be expressed in terms of the following series combinations:

$$
\begin{aligned}
W &= \sum_{n=1}^{\infty} W_{\zeta n}(\zeta)\sin n\pi\eta + \sum_{m=1}^{\infty} W_{\eta m}(\eta)\sin m\pi\zeta + \sum_{m=1}^{\infty}\sum_{n=1}^{\infty} W^*_{mn}\sin m\pi\zeta\sin n\pi\eta \\
\Phi &= \sum_{n=1}^{\infty} \Phi_{\zeta n}(\zeta)\sin n\pi\eta + \sum_{m=1}^{\infty} \Phi_{\eta m}(\eta)\sin m\pi\zeta + \sum_{m=1}^{\infty}\sum_{n=1}^{\infty} \Phi^*_{mn}\sin m\pi\zeta\sin n\pi\eta
\end{aligned}
\tag{22}
$$

where $W_{\zeta n}(\zeta)$, $W_{\eta m}(\eta)$, $\Phi_{\zeta n}(\zeta)$, $\Phi_{\eta m}(\eta)$ are unknown functions, and W^*_{mn}, Φ^*_{mn} are unknown constants.

Substituting Eq. (22) into Eq. (19) and expressing Q, Q_N, Q_M, F_1, F_1', F_2 and F_2' into the following Fourier series form

$$
\begin{aligned}
Q &= \sum_{m=1}^{\infty}\sum_{n=1}^{\infty} Q_{mn} \sin m\pi\zeta \sin n\pi\eta \\
Q_N &= \sum_{m=1}^{\infty}\sum_{n=1}^{\infty} Q_{Nmn} \sin m\pi\zeta \sin n\pi\eta \\
Q_M &= \sum_{m=1}^{\infty}\sum_{n=1}^{\infty} Q_{Mmn} \sin m\pi\zeta \sin n\pi\eta \\
F_1 &= \sum_{m=1}^{\infty}\sum_{n=1}^{\infty} F_{1mn} \sin m\pi\zeta \sin n\pi\eta \\
F_1' &= \sum_{m=1}^{\infty}\sum_{n=1}^{\infty} F_{1mn}' \sin m\pi\zeta \sin n\pi\eta \\
F_2 &= \sum_{m=1}^{\infty}\sum_{n=1}^{\infty} F_{2\,mn} \sin m\pi\zeta \sin n\pi\eta \\
F_2' &= \sum_{m=1}^{\infty}\sum_{n=1}^{\infty} F_{2\,mn}' \sin m\pi\zeta \sin n\pi\eta
\end{aligned}
\tag{23}
$$

we can obtain ordinary differential equations in $W_{\zeta n}(\zeta)$, $W_{\eta m}(\eta)$, $\Phi_{\zeta n}(\zeta)$, $\Phi_{\eta m}(\eta)$ and algebraic equations in Φ_{mn}^*, W_{mn}^*:

$$
\begin{aligned}
&W_{\zeta n}^{(4)}(\zeta) - 2v_d(\lambda n\pi)^2 W_{\zeta n}^{(2)}(\zeta) + (\lambda n\pi)^4 W_{\zeta n}(\zeta) = 0 \\
&\lambda^4 W_{\eta m}^{(4)}(\eta) - 2v_d(\lambda m\pi)^2 W_{\eta m}^{(2)}(\eta) + (m\pi)^4 W_{\eta m}(\eta) = 0 \\
&(m^2 + \lambda^2 n^2)^2 \pi^4 W_{mn}^* = Q_{mn} + F_{2\,mn} + \varepsilon_b F_{2\,mn}' - Q_{M\,mn} \\
&\Phi_{\zeta n}^{(4)}(\zeta) - 2v_a(\lambda n\pi)^2 \Phi_{\zeta n}^{(2)}(\zeta) + (\lambda n\pi)^4 \Phi_{\zeta n}(\zeta) = 0 \\
&\lambda^4 \Phi_{\eta m}^{(4)}(\eta) - 2v_a(\lambda m\pi)^2 \Phi_{\eta m}^{(2)}(\eta) + (m\pi)^4 \Phi_{\eta m}(\eta) = 0 \\
&(m^2 + \lambda^2 n^2)^2 \pi^4 \Phi_{mn}^* = \varepsilon_a(F_{1\,mn} - \varepsilon_b F_{1\,mn}') - Q_{N\,mn}
\end{aligned}
\tag{24}
$$

The solution to Eq. (24), in conjunction with some boundary conditions, can be obtained without much difficulty. If $F_{1\,mn}$, $F_{1\,mn}'$, $F_{2\,mn}$ and $F_{2\,mn}'$ are taken as constants, the solution to Eq. (24) can be obtained immediately. Once these functions as well as the constants in equation Eq. (22) are determined, the functions W and Φ can be obtained.

The problem is that $F_{1\,mn}$, $F_{1\,mn}'$, $F_{2\,mn}$ and $F_{2\,mn}'$ are functions of W and Φ. However, if the coefficients Q_{mn}, $F_{2\,mn}$ and $F_{2\,mn}'$ are given, the function W can be obtained by the aforementioned method. Once $F_{1\,mn}$ and $F_{1\,mn}'$ are determined, then Φ can be obtained. The load Q, and the thermal load Q_N and Q_M are determined for a case involving transverse loads and one-dimensional temperature field. In this case, the coefficients Q_{mn}, $Q_{N\,mn}$ and $Q_{M\,mn}$ defined by the expression (23) are determined. At first, an initial value $W^{(0)}$ is assigned to W, then the functions F_1 and F_1' in Eq. (19) can be obtained and coefficients $F_{1\,mn}$ and $F_{1\,mn}'$ in Eq. (23) are obtained. This leads to the first approximate value $\Phi^{(0)}$ of Φ. When $W^{(0)}$ and $\Phi^{(1)}$ are determined, functions F_2 and F_2' in Eq. (19) can be obtained, and then the first approximate value $W^{(1)}$ of W can be determined. This is continued until we develop a series of approximate solutions for $W^{(1)}$, $\Phi^{(1)}$; $W^{(2)}$, $\Phi^{(2)}$; $\ldots$ $W^{(n-1)}$, $\Phi^{(n-1)}$; $W^{(n)}$, $\Phi^{(n)}$ by the nth iteration. If the difference between the solutions of the $(n-1)$th and nth is within an assumed tolerance of 10^{-4}, we accept the values of W and Φ as being the solution.

Once these functions are determined, the stress and moment resultants, stresses and strains of the shell under transverse loading can be found. This will enable us to determine the large deflections experienced by the shell.

4. Numerical results and discussion

The solution of Eq. (19) was carried out using N terms Fourier series. The number of terms N needed for convergence was carefully examined. For example, the centre deflection of a square plate W is 4.7853 for $N = 5$ and 4.7381 for $N = 7$ under uniform lateral load $Q = 400$. Furthermore, the maximum dimensionless stress at the plate centre is 9.3931 for $N = 5$ and 9.2183 for $N = 7$, respectively. For the sake of convenience, the number of terms in this series N was limited to seven in our analysis.

To validate the solution, the results of our analysis for a simply supported square isotropic plate under uniform lateral load are compared with Brown and Harvey (1969) in Fig. 2. The centre deflection is shown in Fig. 2(a), and the results of corresponding membrane and bending stresses are depicted in Fig. 2(b). The comparisons show good agreement between the two.

The analysis of the FG plates and shells was conducted for two types of ceramic and metal combinations. The first set of materials considered was zirconia and aluminum. The second one was a combination of alumina and aluminum. Young's modulus, Poisson's ratio, thermal conductivity and coefficient of thermal expansion were selected as being 70 GPa, 0.3, 204 W/mK, $23.0 \times 10^{-6}/°C$ for aluminum; 380 GPa, 0.3, 10.4 W/mK, $7.4 \times 10^{-6}/°C$ for alumina, and 151 GPa, 0.3, 2.09 W/mK, $10.0 \times 10^{-6}/°C$ for zirconia, respectively. In all cases, the lower surface of the shell is assumed to be metal (aluminum) rich and the upper surface is assumed to be pure ceramic (alumina or zirconia). In this analysis, only nonlinear elastic behavior of the FG plates and shells was considered.

The analytic results are presented in terms of dimensionless deflection and stress. The dimensionless parameters used are as follows:

centre deflection $W = w/h$,
load parameter $Q = q_0 a^4/(E_m h^4)$,
bending moment $M = M_x a^2/(E_m h)$,
axial stress $\sigma = \sigma_x a^2/(E_m h^2)$,
thickness coordinate $Z = \xi/h$,

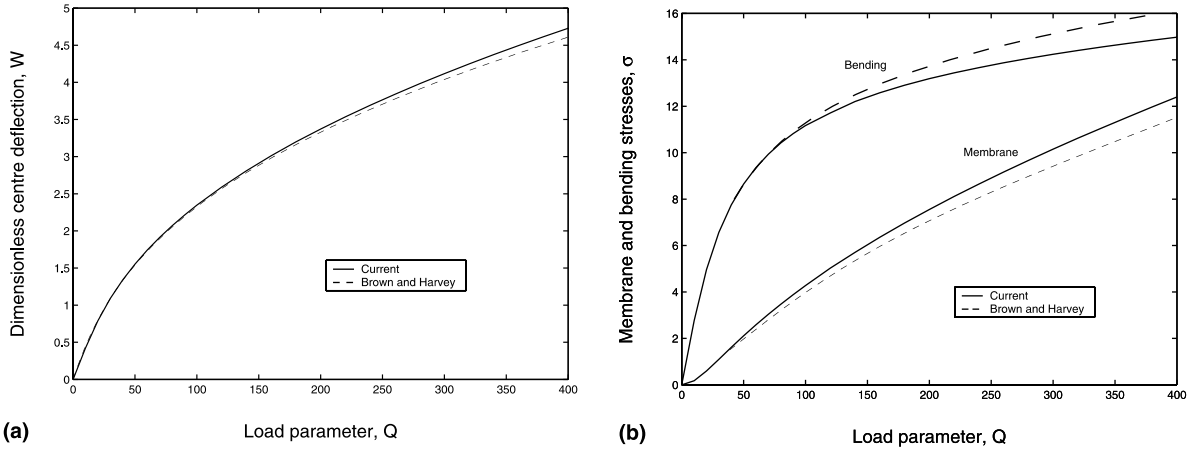

Fig. 2. Validation of results using simply supported square isotropic plate: (a) central deflection versus uniform lateral pressure, and (b) membrane and bending stresses in x-direction at the centre of the plate versus lateral pressure.

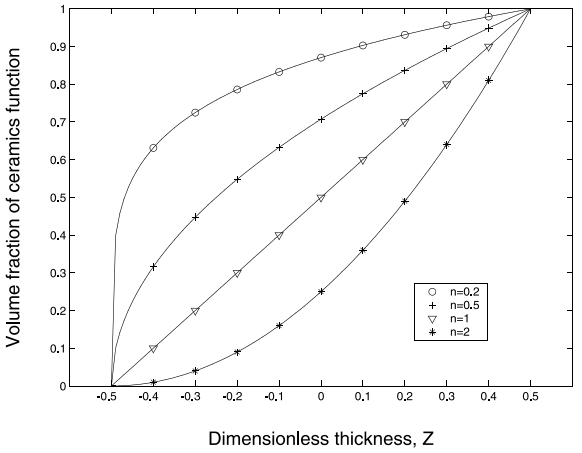

Fig. 3. Variation of the volume fraction $(Z+0.5)^n$ through the dimensionless thickness Z.

where E_m is Young's modulus of the metal used in the functionally graded material, q_0 is a uniformly distributed load, a is the projected length of the shallow shell in the xy plane, and h is the thickness of that shell. The analysis was performed on square shells of side $a = b = 0.2$ m and thickness $h = 0.01$ m.

Fig. 3 shows the volume fraction of the ceramic phase through the dimensionless thickness. Fig. 4(a) shows the central deflection due to a mechanically applied load Q for four simply supported square aluminum–almina plates. Under the same load, the pure aluminum plate has the largest central deflection. This is due to the fact that it has the lowest Young's modulus E_m. Even though the FGM plate $(n = 2)$ contains a small volume fraction of alumina, it is much stiffer than the pure aluminum plate. Fig. 4(b) shows the variation of a dimensionless axial stress σ across the thickness Z at the centre of the four plates investigated due to a load parameter $Q = -400$. The stress distribution in the aluminum and alumina plates is linear; whereas, for the functionally graded composite material, the behavior is nonlinear and is governed by the variation of the properties in the thickness direction.

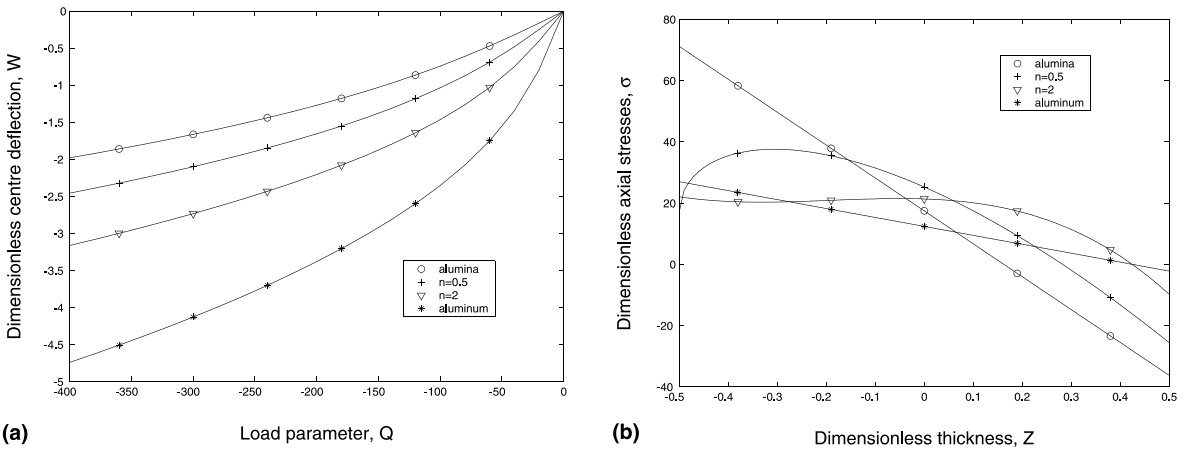

Fig. 4. Nonlinear behavior of FGM plates for various values of volume fractions (aluminum–alumina) of the plates: (a) dimensionless central deflection versus uniform transverse load, and (b) dimensionless axial stress σ along the thickness Z at the center of the plates under the load $Q = -400$.

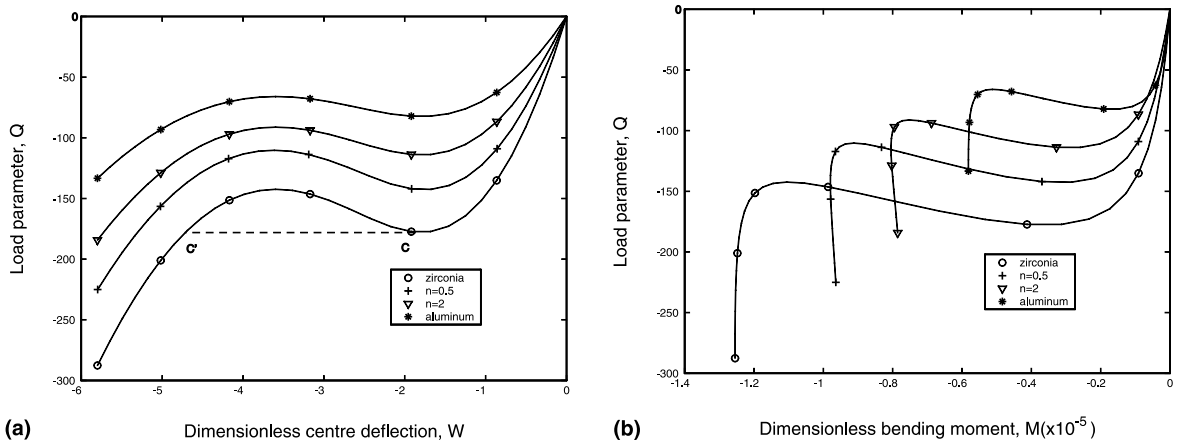

Fig. 5. Nonlinear behavior of FGM shallow spherical shells ($R = R_\zeta = R_\eta = 1$) with various values of volume fractions (aluminum–zirconia): (a) dimensionless central deflection versus uniform transverse load, and (b) dimensionless bending moment M at the center of the shells versus uniform transverse load.

Let us define $R_\zeta = R_x/a$ and $R_\eta = R_y/a$ in the case involving shallow shells. The central deflection versus uniform transverse load for the square shallow spherical shells ($R = R_\zeta = R_\eta = 1$) is shown in Fig. 5(a). The stiffness of the shells, or the slope of the load–deflection curve, decreases with increasing load. At the critical load Q_c, corresponding to point C, the load–deflection curve reaches a zero slope. If the load is maintained as the shell deforms, the central deflection snaps from C to C′. The snap-through buckling of shallow shell occurs at this position. Fig. 5(b) shows the central bending moment M versus the load for spherical shells. The phenomenon of snap-through buckling can also be found through the load and bending moment curves.

Fig. 6 shows the influence of various radii of curvature ($R = \infty$, 5, 2, 0.725) of square spherical shells made of FGM ($n = 1$) on the load–deflection curves. The shell with a smaller initial radius has a higher stiffness at the beginning of deformation. However, the stiffness decreases more rapidly, and if the slope of the load–deflection curve reaches zero, the shell will ultimately buckle.

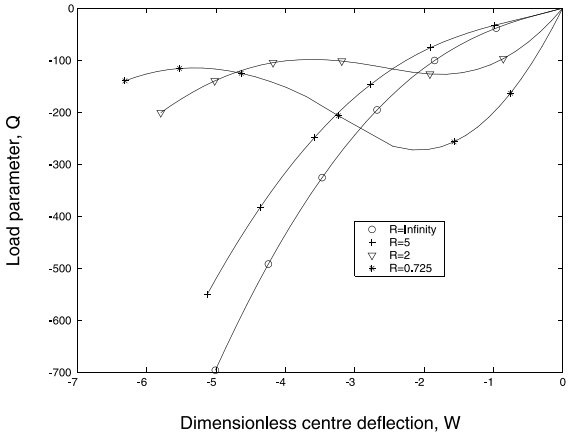

Fig. 6. Dimensionless central deflection versus applied uniform transverse load for shallow spherical shells of various radii of curvature ($R = \infty$, 5, 2, 0.725) with $n = 1$ (aluminum–zirconia).

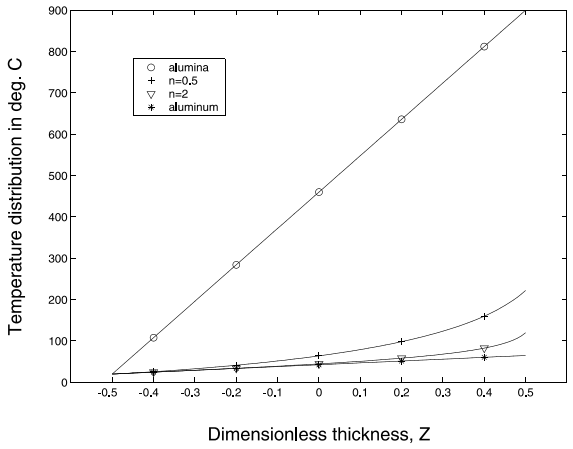

Fig. 7. Temperature field through the thickness of the FGM plates (aluminum–alumina) for the assumed temperature field.

Let us now consider the influence of a temperature field on the behavior of the functionally graded composite. In the present analysis, in addition to the uniform loading, the plate is subjected to a one-dimensional temperature field, where the lower surface was held at a prescribed temperature of 20°C and the heat flow from the upper surface to the lower one was assumed to be 9.152×10^5 W/m^2. The initial stress free state is assumed to exist at a temperature of $T_0 = 0$°C. Fig. 7 shows the temperature distribution through the thickness of the aluminum–alumina plates for various values of the volume fraction exponent n. For the pure alumina and aluminum plates, the temperature at the upper surface is 900°C and 64.9°C, respectively. Now that the temperature field distribution is obtained, the thermal force N^{T} and thermal moment M^{T} can be calculated using Eq. (14). The solution of the coupled equations given by Eq. (19) under mechanical loading and a temperature field can then be obtained using the aforementioned method.

Fig. 8 shows the centre deflection of the aluminum–alumina plates due to a mechanical load and a temperature field. The deflection of the functionally graded plates is positive, when they are subjected to the thermal load. This is due to the fact that the thermal expansion $\alpha\Delta T$ at the upper surface is larger than that experienced by the lower surface.

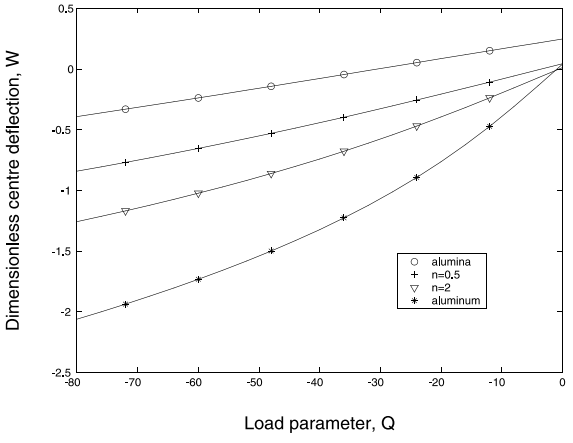

Fig. 8. Dimensionless central deflection under uniform transverse load and temperature field for FGM plates with various values of volume fractions (aluminum–alumina).

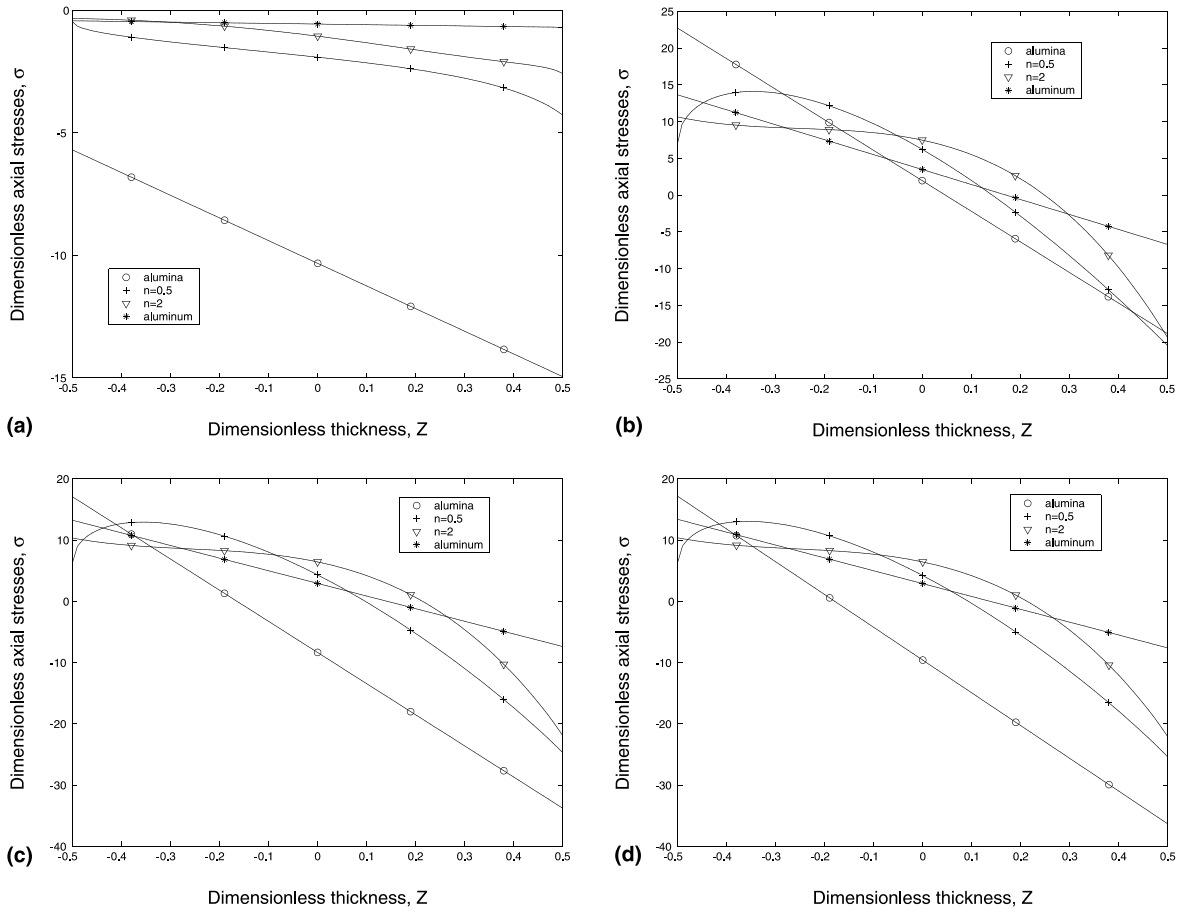

Fig. 9. Dimensionless axial stress σ along the thickness Z at the centre of the plates for FGM plates with various values of volume fractions (aluminum–alumina) due to: (a) temperature field only, (b) mechanical load $(Q = -80)$ only, (c) algebraic sum of thermal and mechanical loadings, (d) coupled thermomechanical loading.

Fig. 9 shows the variation of the dimensionless axial stresses σ along the dimensionless thickness Z at the center of the plates under three different loading cases. Fig. 9(a) shows the results due to the temperature field only and Fig. 9(b) shows the stress distribution due to the mechanical load with $Q = -80$. Fig. 9(c)–(d) shows the variation of stresses under combined thermomechanical loadings. In Fig. 9(c), the stresses were obtained by merely adding the components algebraically. However, this does not account for the coupling effects present in the current nonlinear problem. Fig. 9(d) shows the results when coupling effects were considered. The results show that an increase of 7.59% in the dimensionless compressive stress at the upper surface of the alumina plate as a result of coupling effects.

5. Conclusion

The large deflection of plates and shallow shells made of FGMs under transverse loads is studied. The fundamental equations for shallow thin rectangular shells of FGM have been obtained using the von

Karman theory for large transverse deflections. The material properties of FGM shells are assumed to vary continuously through the thickness of the shell, and were graded according to a power law distribution of a volume fraction of the constituents. A series solution is used to solve the nonlinear equations under general combined thermomechanical loading. Dimensionless deflection, stresses and bending moments were computed for two different combinations of functionally graded plates and shallow shells. The results reveal the marked influence of the constituents upon the field variables for the different types of mechanical and thermal loads considered.

References

Brown, J.C., Harvey, J.M., 1969. Large deflections of rectangular plates subjected to uniform lateral pressure and compressive edge loading. J. Mech. Engng. Sci. 11, 305–317.

Feldman, E., Aboudi, J., 1997. Buckling analysis of functionally graded plates subjected to uniaxial loading. Composite Structures 38, 29–36.

Gould, P.L., 1977. Static analysis of shells. D.C. Heath and Company, Lexington, Massachusetts.

Ishikawa, T., 1990. Thermal deformation and thermal stress of FGM plates under steady graded temperature field, Proc. 1st Int. Symp. on FGM, Sendai, Japan, 11–25.

Loy, C.T., Lam, J.N., Reddy, J.N., 1999. Vibration of functionally graded cylindrical shells. Int. J. Mech. Sci. 41, 309–324.

Miyamoto, Y., 1999. Functional graded materials: design, processing and applications Kluwer Academic Publishers, Boston, Massachusetts.

Obata, Y., Noda, N., 1994. Steady thermal stresses in a hollow circular cylinder and a hollow sphere of a functionally graded material. J. Thermal Stresses 17, 471–487.

Praveen, G.V., Reddy, J.N., 1998. Nonlinear transient thermoelastic analysis of functionally graded ceramic-metal plates. Int. J. Solids Struct. 35, 4457–4476.

Takezono, S., Tao, K., Inamura, E., Inoue, M., 1996. Thermal stress and deformation in functionally graded material shells of revolution under thermal loading due to fluid. JSME Int. J., Series A: Mech. Mater. Engng. 39, 573–581.

Tanaka, K., Tanaka, Y., Watanabe, H., Poterasu, V.F., Sugano, Y., 1993. Improved solution to thermoelastic material design in functionally graded materials: scheme to reduce thermal stresses. Comp. Meth. Appl. Mech. Engng. 109, 377–389.

Wetherhold, R.C., Seelman, S., Wang, J., 1996. Use of functionally graded materials to eliminate or control thermal deformation. Compos. Sci. Technol. 56, 1099–1104.